frontiers | Frontiers in Earth Science

TYPE Original Research
PUBLISHED 11 August 2022
DOI 10.3389/feart.2022.932843

OPEN ACCESS

EDITED BY
Yihong Duan,
Chinese Academy of Meteorological Sciences, China

REVIEWED BY
Jinjie Song,
Chinese Academy of Meteorological Sciences, China
Jingliang Huangfu,
Institute of Atmospheric Physics (CAS), China

*CORRESPONDENCE
Qinglan Li,
ql.li@siat.ac.cn

SPECIALTY SECTION
This article was submitted to Atmospheric Science, a section of the journal Frontiers in Earth Science

RECEIVED 30 April 2022
ACCEPTED 14 July 2022
PUBLISHED 11 August 2022

CITATION
Li G, Li Q, Zhao W, Zhou G, Qian Q, Qian C and He L (2022), Enhanced understanding of changes in tropical cyclones' landfall frequency over mainland China.
Front. Earth Sci. 10:932843.
doi: 10.3389/feart.2022.932843

Enhanced understanding of changes in tropical cyclones' landfall frequency over mainland China

Guangxin Li[1,2], Qinglan Li[1]*, Wei Zhao[1], Guanbo Zhou[3], Qifeng Qian[3], Chuanhai Qian[3] and Lunkai He[1,2]

[1]Shenzhen Institute of Advanced Technology, Chinese Academy of Sciences, Shenzhen, China, [2]University of Chinese Academy of Sciences, Beijing, China, [3]National Meteorological Center, Beijing, China

The climatological characteristics and interannual variations of tropical cyclones (TCs) making landfall in mainland China during the peak TC seasons (July–October) from 1980 to 2020 are examined using the China Meteorological Administration (CMA) best-track dataset. There were 270 TCs landfalling in mainland China during the study period, with 226 TCs landfalling in South China (SC) and 44 TCs landfalling in East China (EC). During 1980–2020, the number of TCs affecting mainland China gradually decreased, although the trend is not significant. The number of TCs impacting SC is experiencing a significant decrease, while the number of TC affecting EC is stable. Based on the change-point analysis, the TC landfall frequency in mainland China and SC incurred significant decreases in 1995/1996 and 1996/1997, respectively. The significant reduction in the number of landfalling TCs over SC and the insignificant reduction in the TC landfall frequency over mainland China are mainly due to the great reduction in the TC formation frequency over the western North Pacific (WNP). Meanwhile, the yearly mean of TCs' landfalling latitudes is moving northward slightly, possibly linked to the slight poleward shift of their genesis locations. A large area of negative anomalies in the lower-tropospheric absolute vorticity and positive variations in the vertical wind shear (VWS) over the tropical WNP are possibly responsible for the reduction in TC genesis over the WNP. Moreover, the apparent opposite anomalies of the two variables over the region north of 20°*N* and south of 20°*N* might contribute to the slight poleward shift of genesis locations of landfalling TCs during the 41 years. The variations in the large-scale steering flow are favorable for more TCs moving northwestward and making landfall in EC than before. Meanwhile, the decrease in TC landfall frequency over mainland China is found to be significantly correlated to the pronounced warming over the tropical Indian Ocean.

KEYWORDS

tropical cyclone, landfall frequency, mainland China, South China, East China

Introduction

Landfalling tropical cyclones (TCs) bring enormous devastation to people and property in coastal areas (Liu et al., 2020; Wang and Toumi, 2021). China is one of the countries most severely affected by TCs in the world, with an average of 9 TCs making landfall every year (Yin et al., 2010; Dong et al., 2015). The historical data for the 2005–2016 period show that TCs affect 36.7 million people annually in China, leading to a mean annual direct economic loss of 69.5 billion Yuan and 254 deaths (Wang et al., 2019). The socioeconomic losses caused by TCs might become more and more pronounced due to recent population growth and economic development in the coastal region (Wu and Wang, 2004; Li et al., 2017). Therefore, investigating the characteristics and variations in the landfalling TCs' activities and understanding the underlying mechanisms are of great significance.

The frequency of TC landfall is considered to be an essential measure of TC landfall activity in a region, and its changes in China have received considerable attention (Liu and Chan, 2003; Li and Duan, 2010; Chan et al., 2012; Zhang et al., 2012; Lu and Zhao, 2013; Liu and Chan, 2017; Liu and Chan, 2020; Liu et al., 2020). Liu et al. (2020) examined the variability of the number of TCs landfalling over the entire mainland China and reported that there was no apparent trend in the landfall frequency of TCs over mainland China during 1980–2018. More studies have been conducted on the variations of TC landfall frequency in individual regions of China (Liu and Chan, 2003; Li and Duan, 2010; Chan et al., 2012; Zhang et al., 2012; Lu and Zhao, 2013; Liu and Chan, 2017; Liu and Chan, 2020). Liu and Chan (2003) examined the TCs making landfall along the SC coast from 1960 to 1999, and found a large annual variation in the number of landfalling TCs. A strong El Niño event tended to reduce the number of landfalling TCs, while more TC landfalls were found in years associated with La Niña events (Liu and Chan, 2003). Liu and Chan (2020) reanalyzed the interdecadal variations in the frequency of TCs landfalling in SC during the period 1975–2018 and reported that the annual frequency showed a tendency to decrease in 1997 and tended to rise again after 2008, which was closely related to the changes in the number of TCs forming over the WNP and the SCS. Chan et al. (2012) found that the frequency of TCs landing in EC experienced significant variations, with periods ranging from centennial to decadal from 1450 to 1949, which were apparently related to the changes in the planetary-scale atmospheric circulations that went through oscillations on various timescales. Liu and Chan (2017) investigated the changes in TC landfalls in East Asia, and found the TC landfall number in Zhejiang and the Korean Peninsula exhibited upward trends, while the number in Guangdong showed a downward trend during the period 1960–2013 (Liu and Chan, 2017). Previous studies were mainly carried out in specific regions. However, few of them focused on investigating the difference and relationship between changes in TC landfall frequency in the individual regions of China (Li et al., 2017; Shan and Yu, 2021).

Regarding the background reason for the TCs' landfall frequency changes in different regions of China, Li et al. (2017) reported a noticeable enhancement in TC landfall frequency over EC during the period 1975–2014, which was due to the significant changes in the large-scale steering flow, characterized by a prominent cyclonic circulation centered over southeast China. In contrast, the changes in the landfall frequency of TCs making landfall in SC were less apparent (Li et al., 2017). Shan and Yu (2021) confirmed the increasing trend in landfall frequency of TCs over EC in recent decades, but reported a decreasing trend in the annual TC landfalls in SC. The opposite variations of TC landfalls in the two adjacent regions were further reported to be phenomenally independent (Shan and Yu, 2021). They attributed the variations to the significant changes in the TC genesis induced by the decreased relative vorticity and increased vertical wind shear over the WNP (Shan and Yu, 2021). However, for two adjacent coastal regions in China, it is hard for the variations in TCs' landfalls in EC and SC to be independent. The above studies mainly focus on the changes in the number of TCs making landfall in various regions of China, and rarely on the variations of their landfall positions. Several studies have revealed a poleward shift in TC activity over the WNP in recent decades, including genesis position and location of lifetime maximum intensity. Therefore, it is worth investigating if there is a similar northward migration in TC landfall positions over mainland China.

In addition, much attention has been placed on how climate change affects WNP TC activity (Liu and Chan, 2003; Goh and Chan, 2010; Chan et al., 2012; Liu and Chan, 2013; Mei et al., 2015). Many studies have shown the remote effects of sea surface temperature (SST) variability in the tropical Indian Ocean (TIO) on WNP TC frequency through changes in the East Asian-WNP monsoon circulation and associated atmospheric factors (Du et al., 2011; Zhan et al., 2011; Zhan et al., 2014; Gao et al., 2020). Several recent studies claimed the dominant contribution of tropical North Atlantic (TNA) SST to WNP TC frequency (Gao et al., 2018; Zhang et al., 2018). Despite no connections having been reported between WNP TC frequency and El Niño–Southern Oscillation (ENSO), a strong modulation of ENSO on TC genesis locations has been well documented, with more (fewer) TCs generated in the southeast quadrant of WNP in El Niño (La Niña) years (Wang and Chan, 2002; Camargo and Sobel, 2005). The Pacific decadal oscillation (PDO) has also been shown to be responsible for WNP TC formation (Liu and Chan, 2013). However, few studies have thoroughly explored the comprehensive relationships between the global SST changes, environmental factors, and variations of the TC landfall frequency over mainland China.

Therefore, this study aims to achieve an overview of the characteristics and changes in the landfalling TCs in China. Furthermore, environmental conditions are investigated to explore the reasons contributing to the observed changes in the TCs' landfalls. The factors include SST, potential intensity

(PI), vertical wind shear (VWS), low-level absolute vorticity, mid-tropospheric moisture, and large-scale steering flow, which are considered to be essential conditions influencing TC activity (Gray, 1975; Chan and Gray, 1982; Holland, 1983; Chan, 1985; Emanuel and Nolan, 2004; Camargo et al., 2007; Korty et al., 2012; Yanase et al., 2012; Murakami et al., 2013; Ling et al., 2016; Torn et al., 2018).

The rest of the article is organized as follows. The second section introduces the datasets and methods employed in the study. The third section reveals the characteristics of landfalling TCs over mainland China. The fourth section investigates the changes in the activities of landfalling TCs. The fifth and sixth sections discuss the possible environmental factors and global SST variations contributing to such changes. A summary is given in the final section.

Data and methods

Data

TCs that made landfall over mainland China, including Hainan Island, are investigated in this study. The TC best-track data for these TCs are obtained from the China Meteorological Administration (CMA) (Ying et al., 2014), which includes the latitude and longitude of the TC center, and TC intensity in terms of the maximum sustained wind (MSW) near the TC center over a period of 2 minutes. For the climatic studies related to TCs landfalling in China, the CMA database may be more accurate and complete than other datasets from different administrations, as there are many more *in situ* observations available in CMA (Ying et al., 2014; Shan and Yu, 2021). Genesis is defined as the first position for a particular TC that attains the intensity of tropical depression. The TC's landfall position is defined as the intersection of the TC's tracks with the coastlines, similar to the study of Fudeyasu et al. (2018). Following previous studies (Kim et al., 2008; Li et al., 2017), the territory of China is subdivided into SC and EC by an artificial boundary line along 25°*N*. As TCs' data are considered more reliable since the introduction of geostationary meteorological satellites in the mid to late 1970s (Kossin et al., 2014), this study focuses on the TCs formed during the peak TC season (July–October) from 1980 to 2020.

The monthly mean reanalysis data of ECMWF Reanalysis v5 (ERA5) at the horizontal resolution of 0.25°× 0.25° from the European Centre for Medium-Range Weather Forecasts (ECMWF) during the period 1980–2020 are used to investigate the large-scale environmental factors surrounding TCs and explore their contributions to the changes in TC activities in this study (Hersbach et al., 2020). The 600-hPa relative humidity is used to represent the mid-tropospheric relative humidity. The sea surface temperature, sea level pressure, temperature, and humidity profiles of the atmosphere are employed to analyze the potential intensity. The wind field is used to calculate the vertical wind shear, absolute vorticity, and background steering flow. The PDO index, the leading PC of monthly SST anomalies in the North Pacific Ocean, is obtained from https://psl.noaa.gov/data/climateindices/list/.

Methods

The PI is a function of environmental conditions that influence the thermodynamic atmosphere-ocean disequilibrium and the TC thermodynamic efficiency, primary sea surface temperatures, and the TC outflow temperatures, and it is the theoretical upper limit of the wind speed of a TC under the current environmental thermodynamic conditions (Emanuel, 1986; Bister and Emanuel, 2002; Gilford et al., 2017). This study explores PI to analyze the thermodynamic environmental reasons for the changes in the TCs' landfall. According to Bister and Emanuel (2002), the computing equation for PI is expressed as follows (equation 1):

$$\mathrm{PI} = \alpha \sqrt{\frac{T_s}{T_0}\frac{C_k}{C_D}\left[\mathrm{CAPE}^* - \mathrm{CAPE}\right]} \tag{1}$$

where T_s is SST; T_0 is the outflow temperature; C_k is the exchange coefficient for enthalpy; C_D is the drag coefficient; $CAPE^*$ is the saturation moist static energy at the sea surface; and $CAPE$ is the moist static energy of the free troposphere.

It is well known that some dynamic factors, such as VWS, play an essential role in TC formation and development (Emanuel, 2000; Wang, 2012; Liu and Chan, 2020). This study estimates the VWS by the vector difference of the horizontal winds between 200 hPa and 850 hPa (Gray, 1968). TC movement is primarily determined by the large-scale environmental steering flow (Holland, 1983; Chen et al., 2011). Following Wu and Wang (2004), this study calculates the steering flow as averaged flow between 850 and 300 hPa.

Student's *t* test is applied to estimate the significance of linear trends in TC activity during 1980–2020 and the difference in the environmental variables and TC genesis region between different periods (Park et al., 2014; Liu and Chan, 2020). To detect a regime shift in climate series, the change-point detection method following Pettitt (1979) is employed. The trends and regime shifts with p-values less than 0.1 are considered significant. In addition, the correlation between two variables is computed by the Pearson correlation coefficient (Wilks, 2006).

Climatological characteristics of landfalling TCs

During the TC peak seasons of 1980–2020, 270 TCs made landfall in mainland China, of which 171 (63.3%) originated in the WNP, and the rest originated in the South China Sea (SCS). Among the 270 landfalling TCs, 226 TCs (83.7%) affected SC, while 44 TCs (16.3%) hit EC. SC suffered five times as many TCs as EC over the study period. Figures 1A and B show the spatial distribution of the annual mean occurrence frequency of TCs

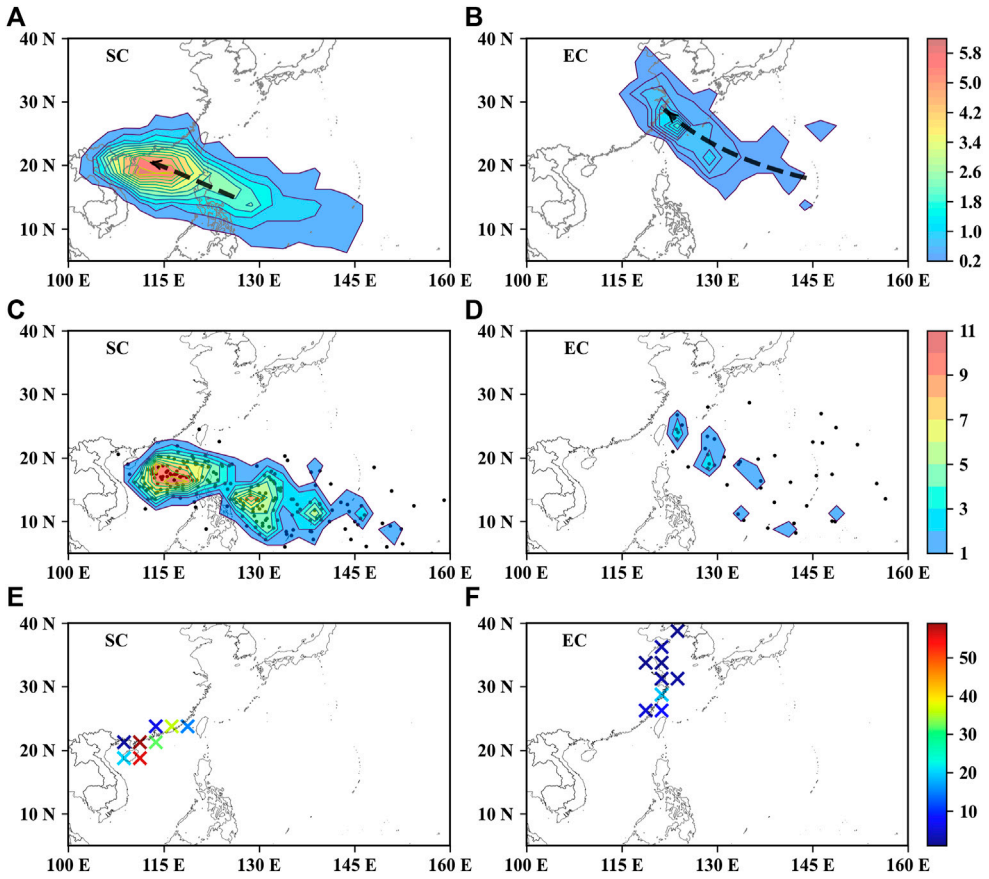

FIGURE 1
Frequency distribution of **(A,B)** annual mean TC occurrence, **(C,D)** TC formation, and **(E,F)** TC landfall over a grid of 2.5°× 2.5° during the TC peak season (Jul–Oct) from 1980 to 2020. The thick dashed curves with arrows in **(A,B)** schematically denote the mean regression trajectories of landfalling TCs, and the markers '.' in **(C,D)** indicate TC genesis locations. The left column is for TCs landfalling in SC and the right column is for TCs landfalling in EC.

affecting SC and EC during 1980–2020. The frequency is counted at each 2.5°× 2.5° grid box. As shown in the figure, most of the landfalling TCs in SC originated over the WNP, passed through the Luzon Strait, entered the SCS, and landed on the southern coast of China. The prevailing track of westward-moving TCs is shown in Figure 1A. For the TCs making landfall over the eastern coast of China, the high frequency of occurrence extended from the WNP to east of Taiwan Island and made landfall in EC, indicating a primary northwestward track (Figure 1B).

The TC genesis locations over SC and EC for the 1980–2020 period are depicted in Figures 1C and D. For the TCs making landfall in SC, approximately half of them (43.8%) formed in the northern part of the SCS, and the rest were generated over the WNP (Figure 1C). As shown, most of the observed genesis locations occur in the tropical belt, between 5°*N* and 20°*N*. Their frequency distribution exhibits two major centers, in the northern SCS and east of the Philippines. The spatial pattern of the formation frequency (Figure 1C) is similar to that of the occurrence frequency (Figure 1A). During the study period, the average genesis location of the TCs landfalling in SC is 14.7°*N*, 126.6°*E*. In comparison, all TCs landfalling in EC originated in the WNP, and most of them formed in the region of 10°*N* – 30°*N*, 120°*E* – 160°*E* with a mean value of 18.5°*N*, 137.2°*E* (Figure 1D). The mean genesis location of TCs landfalling EC is further north and east than that of TCs landfalling SC. The formation distribution of TCs landfalling in SC (Figure 1C) is more concentrated than that of TCs landfalling in EC (Figure 1D).

The spatial distribution of the TCs' landfall frequency over SC and EC during these 41 years is depicted in Figures 1E and F, respectively. The figures show that the TCs' landfalling locations are distributed unevenly along the China coast. The highest landfalling frequency occurs at the grid with the latitude of 20 – 22.5°*N* and longitude of 110 – 112.5°*E* (denoted simply as: at the grid 21.25°*E* , 111.25°*E*; similar expressions are used hereafter). During the study period, 59 TCs landed at this grid. In SC, the lowest landfalling

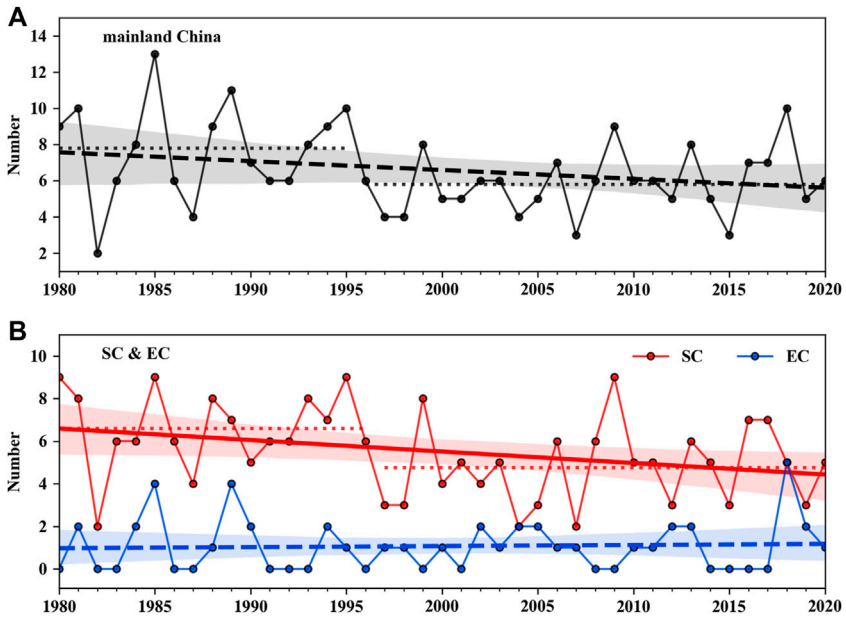

FIGURE 2
The time series and the linear regression fit of the TCs' landfalling frequency over **(A)** mainland China and **(B)** SC and EC from 1980 to 2020. The solid (dashed) trend lines represent significant (insignificant) trends at the 90% confidence level by Student's *t* test. Linear trend lines are shown with their 95% two-sided confidence intervals (shaded). The dotted lines indicate the mean landfall frequency over different periods.

TABLE 1 The linear trends and corresponding *p* values for the annual landfall frequency of TCs over mainland China, SC, and EC from 1980 to 2020.

		Mainland China	SC	EC
Landfall frequency	Trend	−0.049	**−0.054***	0.005
	p value	0.115	0.045	0.760

Values in boldface with an asterisk denote trends that are statistically significant at the 90% confidence level by Student's *t* test.

frequency is at the grid 21.25°*N*, 108.75°*E*, with 2 TCs landfalling during the 41 years. For TCs landfalling in EC, the highest landfalling frequency occurs at the grid 28.75°*N*, 121.25°*E*, with 19 TCs landfalling during the study period. In EC, no TC is found landfalling over three grids, which are [36.25°*N*, 118.75°*E*] [38.7°*N*, 118.75°*E*], and [38.75°*N*, 121.25°*E*], respectively.

Changes in the TC activities

TC landfall

The long-term changes in landfall frequency of TCs in mainland China over the 41-year period are depicted in Figure 2 and Table 1. From 1980 to 2020, the annual number of TCs making landfall in mainland China (including SC and EC) presents an annual mean of 6.6, and its time series show a slight downward trend (Figure 2A and Table 1). Out of them, the number of landfalling TCs in EC is stable, while that in SC presents a significant decreasing trend with a rate of -0.054 per year (Figure 2B and Table 1). The annual frequency of TCs making landfall in SC has reduced by 33.8% over the 41 years, which is the main contribution to the decrease of landfalling TCs in mainland China. These results are somewhat different from several previous conclusions (Li et al., 2017; Shan and Yu, 2021), which suggested an increased frequency of TCs making landfall along the eastern coast of China in recent decades. The possible causes for the divergence in TCs' landfall frequency analysis might be the different study periods and the boundary division line for SC and EC used in these studies.

Based on the Pettitt's test results, as presented in Figure 2, it is clearly shown that the frequencies of TC landfall in mainland China and SC were very likely to change significantly in 1995/1996 and 1996/1997, respectively (with a confidence level of 90%). The mean frequency of TC landfalls over mainland China from 1980 to 1995 is 7.8, whereas the mean frequency from 1996 to 2020 is 5.8. That is, the average number of TC landfalls decreased by approximately 2 after 1995. For TCs landfalling over SC, the average numbers for the periods 1980–1996 and 1997–2020 are 6.6 and 4.8, respectively. The difference between the two periods is 2.2. The apparent drop suggests that large-scale climate factors may have a climate regime shift in the late 1990s, which significantly affects the TC activity in China.

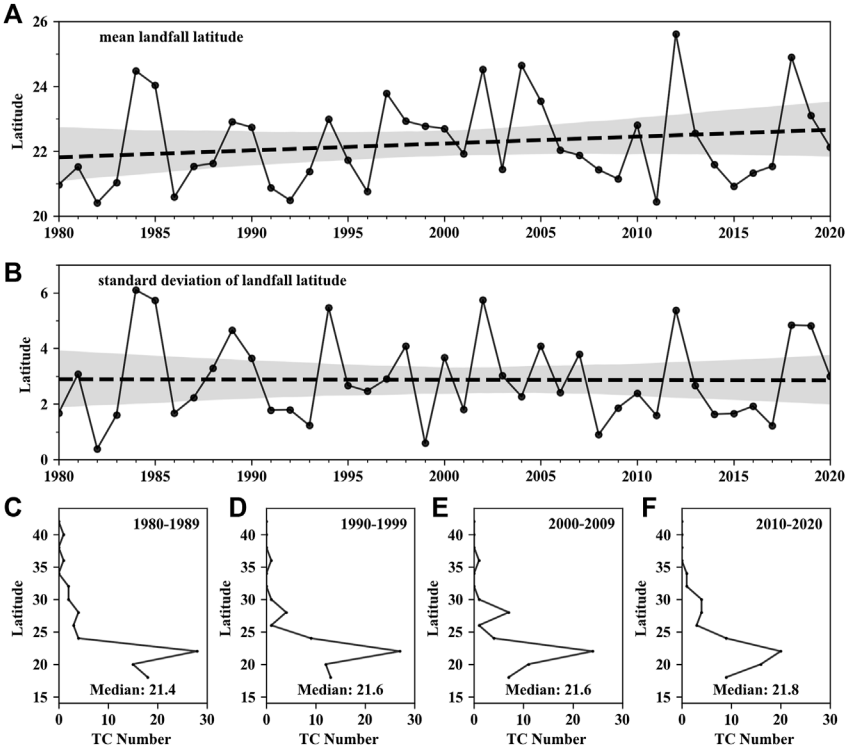

FIGURE 3
The time series and the linear regression fits for **(A)** the annual mean of TCs' landfalling latitudes and **(B)** the standard deviation of the yearly TCs' landfalling latitudes over mainland China from 1980 to 2020. The latitudinal distribution of TCs landfalling over mainland China for the periods: **(C)** 1980–1989, **(D)** 1990–1999, **(E)** 2000–2009, and **(F)** 2010–2020. The medians of the decadal TCs' landfall latitudes are also shown in the corresponding figures.

TABLE 2 The same as Table 1, but for the mean and standard deviation of landfall latitude of TCs over mainland China from 1980 to 2020.

		Mean	Standard deviation
Landfall latitude	Trend	0.021	−0.001
	p value	0.240	0.957

This study further investigates the variation of TCs' landfall locations in terms of the yearly mean of TCs' landfalling latitudes (Figure 3A), the standard deviation (Std) of the yearly TCs' landfalling latitudes (Figure 3B), and the decadal distribution of the TCs' landfalling latitudes over mainland China (Figures 3C–F) from 1980 to 2020. The analysis results are also shown in Table 2. During the study period, the TCs' landfalling latitudes slightly increase (Figure 3A and Table 2), which should be due to the combination of the significant decrease of TC landfalls over SC and unchanged number of TCs affecting EC. As shown in Figures 3B–F, although no obvious changes can be observed in the Std of TCs' landfalling latitude, the latitude range exhibits a decadal decrease during the 41-yr period. The latitudes range for the period of 1980–1989 is from 18.2 °*N* to 39.7 °*N*, while the latitudes range for the period of 2010–2020 is from 18.2 °*N* to 34.6 °*N*. Furthermore, the medians of the TCs' landfall latitudes during the 4 decades (Figures 3C–F) also show a tendency to move northward slightly.

TC genesis

Since a TC landfall is generally considered to be directly relevant to its genesis (Wu and Wang, 2004; Camargo and Sobel, 2005; Park et al., 2013; Shan and Yu, 2021), this study investigates the long-term changes in the formation frequency and location of the landfalling TC from 1980 to 2020 (Figures 4 and 5). The trends and the corresponding *p* values are calculated, and the results are tabulated in Table 3. As shown in Figures 4A and B, for the TCs making landfall over mainland China, the annual number of TCs forming in both the WNP and the SCS changed slightly during these 41 years. As discussed in the previous subsection, all the landfalling TCs over EC form in the WNP, and the total number has no trend over the 41-year period (Figures 4C

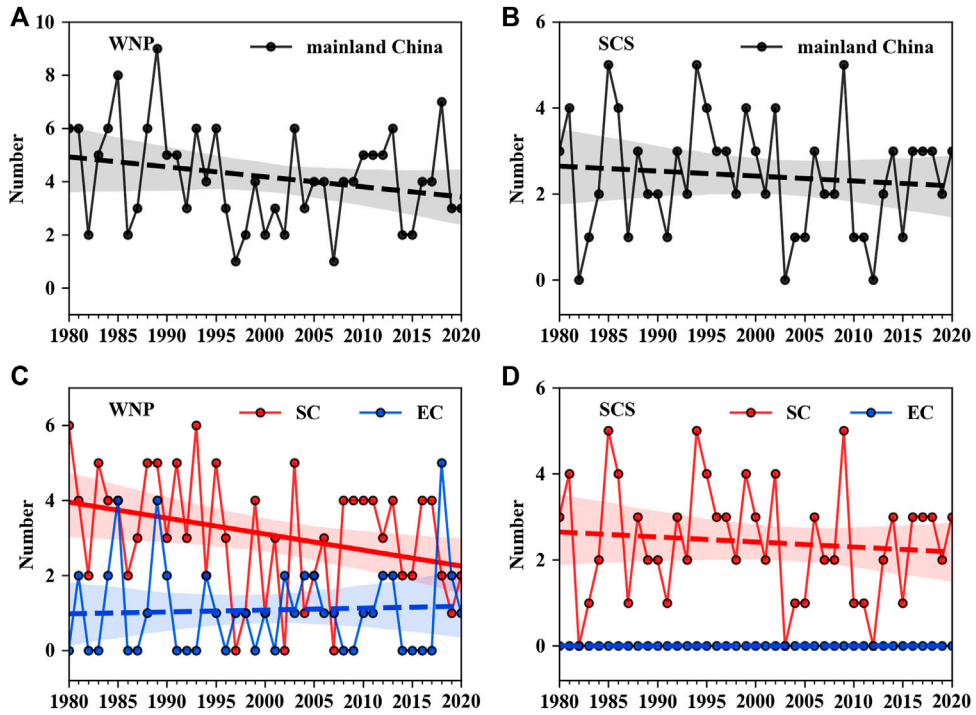

FIGURE 4
The same as Figure 2, but for the annual number of the TCs generated in the WNP **(A,C)** and SCS **(B,D)** and made landfall in mainland China, SC, and EC.

and D and Table 3). As mentioned earlier, nearly half of the landfalling TCs over SC come from the WNP, and the rest generate over the SCS. The former show a significant decrease during 1980–2020, with a mean rate of -0.043 per year (Figure 4C and Table 3). The annual genesis number has decreased by 50% over the 41 years (Figure 4C). The latter shows no apparent changes (Figure 4D and Table 3). Thus, the significant reduction in the total number of landfalling TCs over SC during the 41 years results from the corresponding apparent decrease in the number of TCs formed in the WNP. The correlation coefficient between them is 0.76, and this correlation is highly significant ($p < 0.1$). The slight reduction in TC genesis over the WNP (Figure 4A) might also help explain the decrease in the frequency of TC landfalls over mainland China (Figure 2A), although the decline of TC landfall frequency in mainland China is less apparent than those of TCs over SC.

The shift in TCs' genesis locations also has a significant impact on the TCs' landfall activity in the East Asia region (Yonekura et al., 2014; Liu and Chan, 2017). This study further explores the zonal and meridional changes in the TC formation locations. Figures 5A–D are the time series of the annually averaged genesis latitude and longitude of TCs making landfall in mainland China, SC, and EC from 1980 to 2020. The trends and the corresponding p values for these changes are recorded in Table 4.

Landfalling TCs over mainland China show a slight increment and reduction in their mean genesis latitude and longitude over the 41 years (Figures 5A and B and Table 4). It seems plausible that the increase in genesis latitude of landfalling TCs (Figure 5A) may be one of the reasons for the poleward shift of their landfall positions (Figure 3A). The correlation coefficient between the latitude anomalies of TC landfall and that of TC genesis is 0.6 ($p < 0.1$). From them, the mean genesis latitude of landfalling TCs over SC shows a significant increasing trend, with a rate of 0.041° per year (Figure 5C and Table 4). As shown in Figure 1C, most of the landfalling TCs over SC form in the tropical belt south of 20°N. It indicates that the TC genesis region has a trend away from the equator. Such poleward TC migration is consistent with Studholme et al. (2022), who suggest that more WNP TCs tend to form at higher latitudes, take north-turning tracks, and then occupy a broader range of latitudes. On the other hand, the mean genesis longitude decreases significantly, and the decline rate is -0.133° per year (Figure 5D and Table 4). It suggests that there has been a markedly poleward and westward shift in the genesis region of TCs making landfall over SC during the past 41 years (Figures 5C and D). This might be induced by the

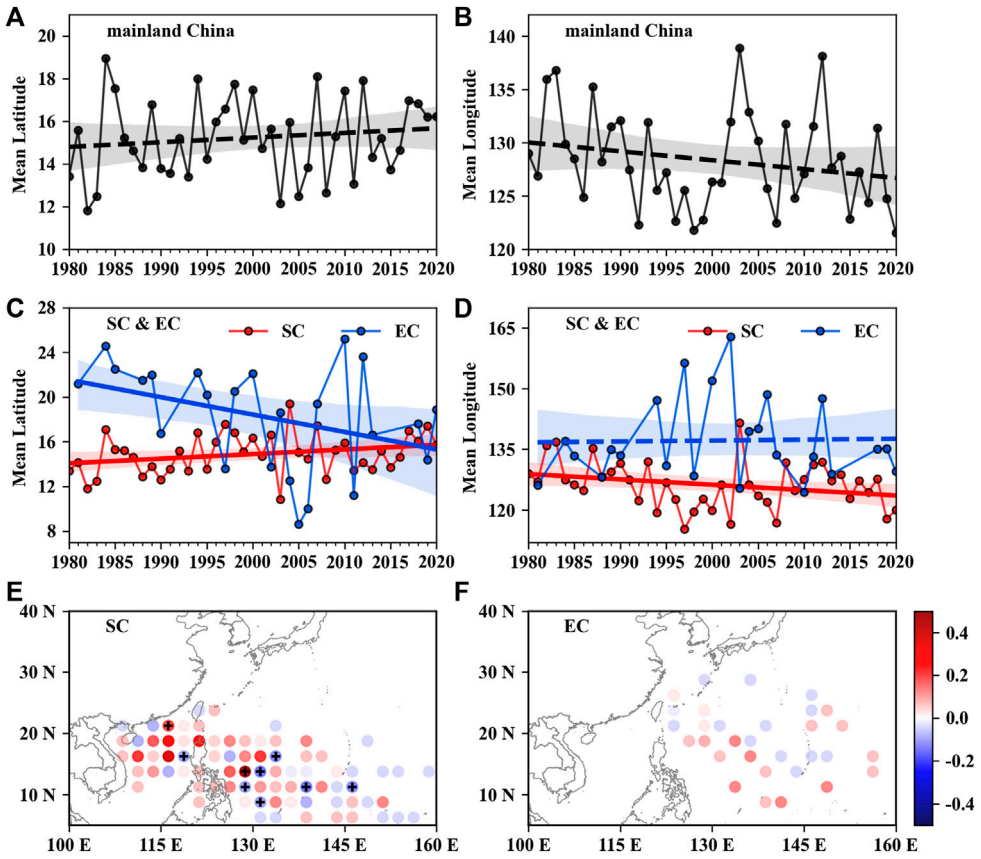

FIGURE 5
The same as Figure 2, but for the annual mean genesis **(A,C)** latitude and **(B,D)** longitude for the landfalling TCs over mainland China, SC, and EC. The difference in the genesis frequency for TCs landfalling over **(E)** SC and **(F)** EC between 1980–1995 and 1996–2020. The marks '+' indicate where the difference between the two periods is significant at a confidence level of 90%.

TABLE 3 The same as Table 1, but for the number of TCs generated in the SCS and WNP and made landfall over mainland China, SC, and EC from 1980 to 2020.

		Mainland China	SC	EC
SCS TCs	Trend	−0.011	−0.011	nan
	p value	0.523	0.523	nan
WNP TCs	Trend	−0.037	**−0.043***	0.005
	p value	0.131	0.044	0.760

Values in boldface with an asterisk denote trends that are statistically significant at the 90% confidence level by Student's t test.

TABLE 4 The same as Table 1, but for the genesis latitude and genesis longitude of TCs over mainland China, SC, and EC from 1980 to 2020.

		Mainland China	SC	EC
Genesis latitude	Trend	0.022	**0.041***	**−0.156***
	p value	0.383	0.082	0.070
Genesis longitude	Trend	−0.083	**−0.133***	0.022
	p value	0.171	0.082	0.908

Values in boldface with an asterisk denote trends that are statistically significant at the 90% confidence level by Student's t test.

significant reduction in the number of TCs forming in the WNP (Figure 4C) and almost no change in the number of TCs forming in the SCS (Figure 4D). In addition, the TCs making landfall in EC tend to generate at a lower latitude significantly (Figure 5C and Table 4), and therefore, these TCs are more likely to land in EC at a lower latitude than before (Figures 3C–F).

As shown in Figure 2, the TC landfall frequency over mainland China experienced a climate shift between 1995 and 1996. We then explore the spatial difference in the TC formation frequency between the two periods: period 1 (1980–1995) and period 2 (1996–2020) (Figures 5E and F). Figure 5E shows that more area (20 grids over the total 26 grids) over the northern SCS experiences an increase in the TCs' genesis frequency. For the genesis region

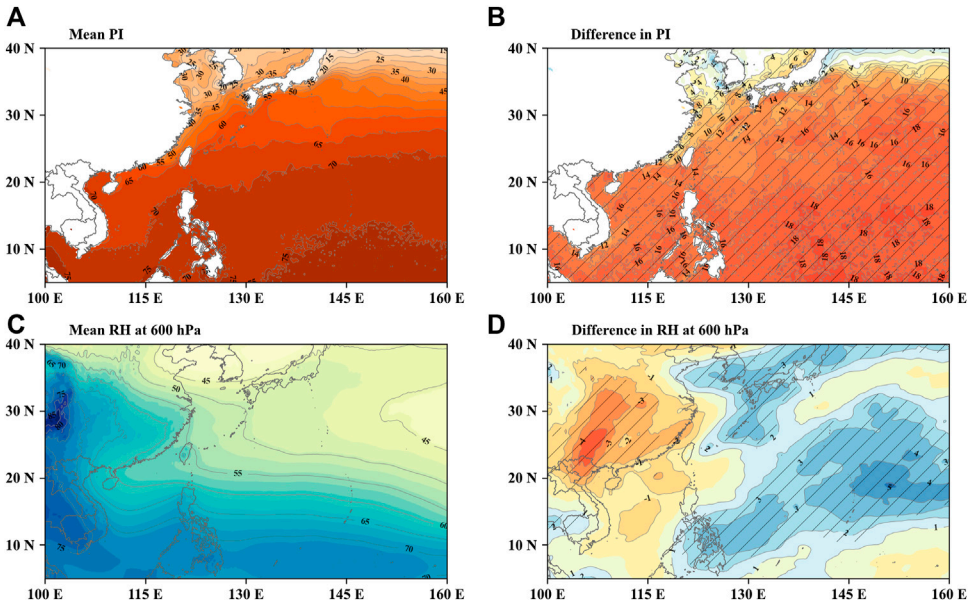

FIGURE 6
The climatological mean from 1980 to 2020 and the difference between 1980–1995 and 1996–2020 for **(A,B)** PI (m s^{-1}) and **(C,D)** RH at 600 hPa (%). The stippling indicates where the difference is significant at a confidence level of 90%.

over the WNP south of 20°*N*, the number of the increasing points (in red) and that of the decreasing points (in blue) are almost the same. However, among those grids for TCs genesis over the WNP (Figure 5E), six points show significant decreasing trends while only one point shows a significant increasing trend. Compared with the anomalies in the SCS, the WNP tends to generate fewer TCs than before. At the same time, a slight increment in the formation frequency of landfalling TCs over EC is observed in the tropical WNP around 10°*N* (Figure 5F). It indicates that more TCs forming in the tropical zone have opportunities to threaten EC. These results also agree with their long-term temporal changes (Figures 5C and D). Thus, the variation of the TCs' landfalling over mainland China in recent decades is mainly related to the changes in the TCs' genesis. Next, we will discuss the environmental reasons for these variations in detail in the following section.

Environmental factors contributing to changes in TCs' landfalls

The activities of TCs are influenced by several dynamic and thermodynamic parameters, including moist static stability and planetary vorticity (Gray, 1975; Emanuel and Nolan, 2004; Camargo et al., 2007; Korty et al., 2012; Yanase et al., 2012; Murakami et al., 2013). For TCs' genesis, the low-level vorticity, relative humidity, the magnitude of VWS between 850 and 250 hPa, and PI are reported to be essential (Gray, 1975; Emanuel and Nolan, 2004; Camargo et al., 2007; Korty et al., 2012). Large low-level vorticity, weak VWS, high PI, and high mid-tropospheric humidity are favorable for TC formation (Camargo et al., 2007; Yanase et al., 2012). To examine the reasons for the recent changes in TCs' genesis, the mean and difference of the large-scale environments surrounding TCs between 1980–1995 and 1996–2020 are analyzed.

PI is a thermodynamic factor considering the influences of both the SST and moist static instability (Bister and Emanuel, 2002; Yanase et al., 2012). Several studies point out that the changes in SST are strongly similar to that of PI over the WNP in recent years (Park et al., 2013; Zhan and Wang, 2017). So, the variations of SST are not discussed independently in this study, although it is a well-known important thermodynamic factor related to TC genesis and development (Emanuel, 1986; Korty et al., 2012). Figures 6A and B present the climatological mean PI for the 41 years and the difference in the mean PI between 1980–1995 and 1996–2020. It is found that the PI gradually increases with the decrease of latitude, and it achieves the highest value in the deep tropics, where the water temperature is also the highest (Figure 6A). As shown in Figures 1C and D, the genesis locations of TCs landfalling in SC are distributed over the region closer to the tropics than those of TCs landfalling in EC. In general, higher PI provides more favorable conditions for TC formation (Yanase et al., 2012). It can partly explain that there are more TCs making landfall in SC than those in EC. As shown in Figure 6B, PI increases significantly over the region south of 35°*N*, covering all the genesis locations of

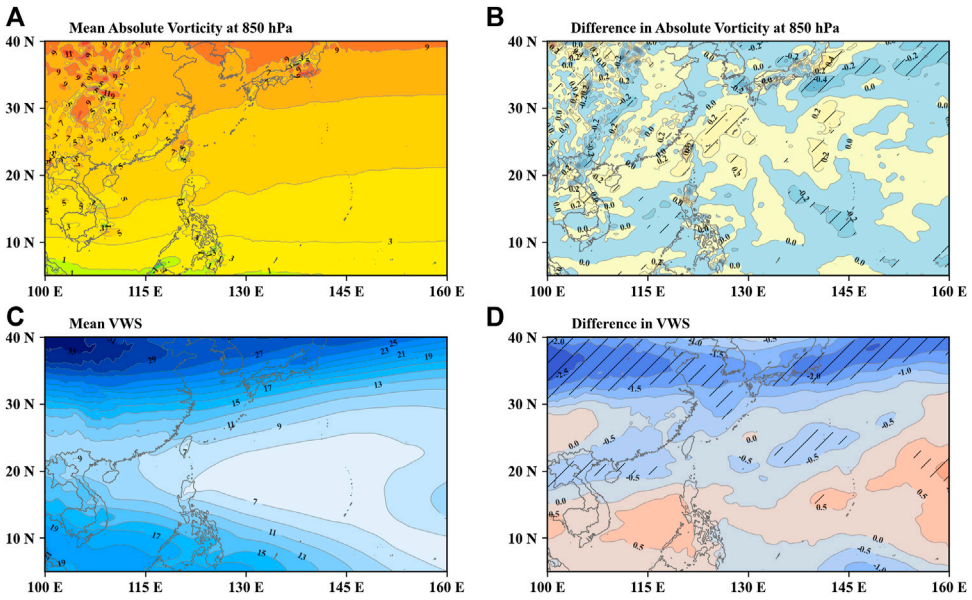

FIGURE 7
The same as Figure 6, but for **(A,B)** absolute vorticity at 850 hPa (10^{-5} s^{-1}) and **(C,D)** VWS (m s^{-1}).

TCs making landfall in mainland China (Figures 1C and D). However, the spatial pattern of PI changes (Figure 6B) cannot explain the decline of TC occurrence over the WNP and the difference in frequency between TCs making landfall in SC and EC (Figures 5E and F).

Usually, high relative humidity (RH) in the middle troposphere is favorable for TC genesis by reducing the detrimental effects of convective downdrafts (Gray, 1975; Korty et al., 2012). Figure 6C shows the mean RH at 600 hPa from 1980 to 2020. Similar to the pattern of PI, the middle troposphere RH in the tropical region is generally greater than that in the subtropical region, and it reaches a maximum of 75% in the deep tropics. It may also explain the long-term difference in the frequencies of TCs making landfall in SC and EC. In Figure 6D, a significant increase in the middle troposphere RH is observed over the region of 10°*N* – 30°*N*, 120°*E* – 160°*E*, covering almost all the genesis regions for TCs affecting EC (Figure 1D). Moreover, the midlevel RH decreases slightly over the northern part of the SCS and increases significantly over the area east of the Philippines, which are the two genesis regions for TCs hitting SC (Figure 1C). However, the changing pattern of the midlevel RH cannot explain the genesis changes for TCs making landfall in SC from 1980 to 2020 (Figure 5E), which are relative stability in the TCs genesis number over the SCS and a significant reduction in the WNP. In summary, the variations of thermodynamic factors, PI and midlevel RH, do not contribute clearly to the changes in the genesis of landfalling TCs over mainland China.

Besides thermodynamic factors, TC genesis is also related to dynamic conditions, such as the lower-tropospheric absolute vorticity and VWS. Many studies stated that the low-level absolute vorticity is necessary for TC genesis, as TCs rarely form within a few degrees of the equator (Gray, 1975; Tippett et al., 2011). Furthermore, most of the cyclogeneses tend to occur around the positive anomaly of absolute vorticity (Gray, 1975; Yanase et al., 2012). Figures 7A and B show the mean absolute vorticity at 850 hPa during the 41 years and the mean absolute vorticity differences between 1980–1995 and 1996–2020. Figure 7A shows that the climatological mean absolute vorticity increases with the latitude, while both RH and PI decrease with the latitude (Figures 6A and C). On average, the largest absolute vorticity values can be found at high latitudes, where few TCs form due to the low SST (Tippett et al., 2011).

To the north of 15°*N*, the absolute vorticity appears to have slight positive anomalies over the northern part of the SCS (Figure 7B), where approximately half of landfalling TCs in SC form (Figure 1C). According to Gray (1975) and Yanase et al. (2012), these positive changes are conducive to TCs' genesis. It possibly contributes to the increase in the TC genesis frequency over the SCS north of 15°*N* (Figure 5E). The absolute vorticity over the waters east of Taiwan Island between 20°*N* and 30°*N* displays an increasing change, and some sporadic regions west of 145°*E* increase significantly (Figure 7B). As shown in Figure 1D, a minority of landfalling TCs in EC form in this region, which could provide favorable vorticity conditions. In comparison, a large area of negative anomalies over the tropical WNP and significant decline over the waters southwest of the Mariana Islands with the longitude range of 140°*E* – 145°*E* are observed, indicating lower absolute vorticity in these areas. These changes

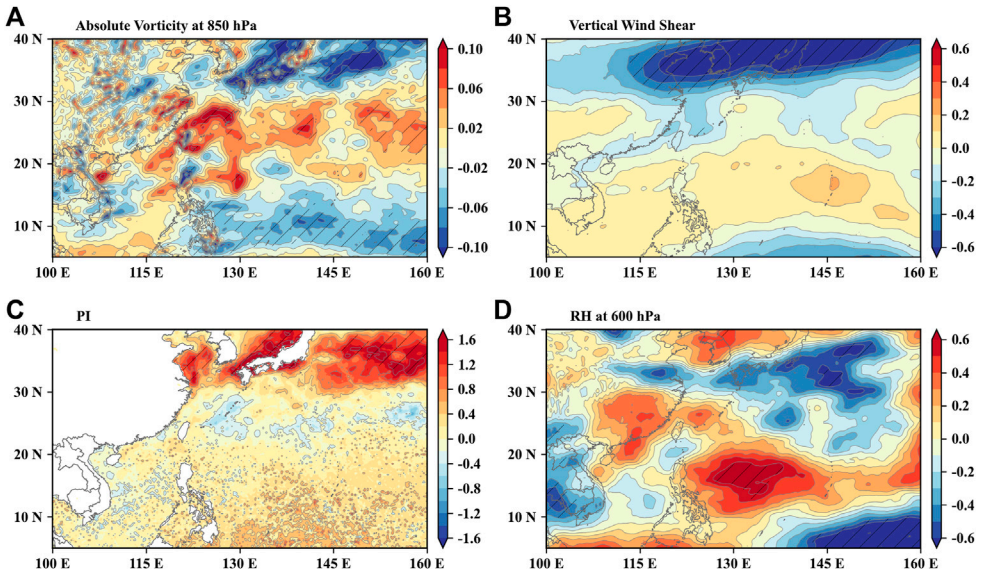

FIGURE 8
Regression of environmental factors with respect to the mean TCs genesis latitudes during 1980–2020. **(A)** Absolute vorticity at 850 hPa (10^{-5} s^{-1} per latitudinal degree), **(B)** VWS (m s^{-1} per latitudinal degree), **(C)** PI (m s^{-1} per latitudinal degree), and **(D)** RH at 600 hPa (% per latitudinal degree). The stippling indicates the regression exceeding the 90% confidence level.

affect the main region of genesis for TCs landfalling over mainland China (Figures 1C and D, Figures 5E and F) and are possibly responsible for the overall decrease in the formation frequency of TCs over the WNP.

It is known that weak VWS is a necessary dynamic condition for tropical cyclogenesis because strong shear will break the warm core structure of the TCs (Gray, 1975; Yanase et al., 2012). The 41-years' climatological mean and difference in the VWS between the two periods are investigated and shown in Figures 7C and D. As depicted in Figures 1C and D, most of the landfalling TCs tend to form in the tropical WNP in the latitude range of $10°N - 25°N$ due to relatively small VWS in this region (Figure 7C). However, the VWS increases in the majority of this region and rises significantly in the east of the Mariana Islands around $[20°N, 160°E]$ after 1995 (Figure 7D). Although the VWS over the northern SCS and the areas east of Taiwan Island present significant decreasing trends, the upward anomalies in VWS over the tropical WNP affect the main genesis region of landfalling TCs and suppress the TCs' formation there.

Comparing Figures 7B and D, the spatial distribution of unfavorable changes in the VWS is similar to that of the decrease in absolute vorticity in the lower troposphere. The reduction in TCs' genesis over the WNP is mainly due to the combination of the increasing VWS and decreasing lower-tropospheric absolute vorticity. Indeed, the thermodynamic factors (PI and RH) over the WNP increased during the 41 years (Figures 6B and D), but the frequency of TC genesis still declined. It means that the dynamic factors are more effective than the thermodynamic conditions in influencing TCs' formation when the thermodynamic conditions are favorable for TCs' genesis. That is, the dynamic factors played a major role in TC genesis in the WNP during the study period. These results are consistent with the previous conclusions of Murakami et al. (2013), who found that dynamic variables are of primary importance for separating developing and non-developing disturbances for TC formation in the present climate of the WNP.

To further identify the relative contributions of the aforementioned environmental factors to the changes in TC genesis latitude, the factors are regressed onto the mean genesis latitude of landfalling TCs over mainland China during 1980–2020 (Figure 8). As shown in Figure 8A, the regression of the 850-hPa absolute vorticity shows significant positive (negative) correlations at the region north (south) of $20°N$, which are favorable (unfavorable) for TC genesis. It suggests that the increase in the mean latitude of TC genesis (Figure 5A) may be related to the variations in the low-level atmospheric absolute vorticity (Figure 7B). Such a result is similar to that found by Wu et al. (2020), who found that the low-level relative vorticity is mainly responsible for the observed increasing variation of mean TC genesis latitude over the WNP. Concurrently, a similar dipole structure can be observed in the regression of VWS (Figure 8B), but the signals are not significant. For the other two environmental conditions (Figures 8C and D), no obvious difference is observed between their regressions at higher and at lower latitudes, or the changes are unfavorable for the poleward shift of TC genesis. In comparison, the low-level atmospheric absolute vorticity and VWS possibly make a relatively more significant contribution to the slight poleward

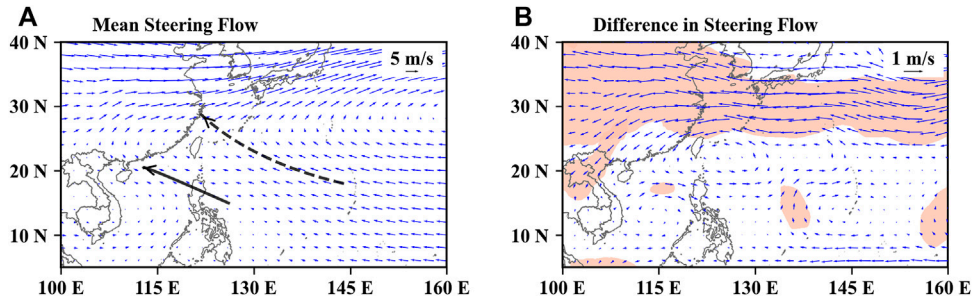

FIGURE 9
The same as Figure 6, but for the Steering Flow (m s^{-1}). The thick black solid (dashed) curves with arrows in **(A)** schematically denote the mean regression trajectories of TCs making landfall in SC (EC). The shaded area in pink **(B)** refers to the difference being significant at a confidence level of 90%.

shift in the TCs' genesis locations than other factors. This also confirms the major role of dynamic factors in the TC genesis over the WNP during the study period.

After genesis, the landfall of a TC is determined by its movement, which is mainly controlled by the large-scale environmental steering flow and also affected by other factors, such as beta shift (Chan and Gray, 1982; Holland, 1983; Chan, 1985; Ling et al., 2016; Torn et al., 2018). This section explores the long-term mean background steering flow and the difference in steering flow between the two periods (Figures 9A and B). It can be seen that the higher the latitude, the stronger the mean steering flow. The westward steering flow in the tropics leads most of the TCs formed in the tropical WNP (including the SCS) to move westward and then make landfall in SC. The remaining TCs formed at higher latitudes hit EC under the strong westerly flow in the midlatitudes (Figure 9A). After the TCs' landfall in EC, they may reenter the sea at an even higher latitude, controlled by the steering flow, if they do not dissipate in the mainland (Figure 9A).

In Figure 9B, the large-scale steering flows over the Philippine Sea are characterized by a cyclonic anomaly centered over the waters east of Taiwan Island. This cyclonic anomaly presents an anomalous westerly flow in the latitude band between 10°*N* and 20°*N*, suppressing the movement of TCs from the Philippine Sea to the SCS and reducing the chance of TCs making landfall along the SC coast. That means, with the depression of TCs' activity, the number of TCs making landfall along the SC coast is, therefore, reduced. Concurrently, the significant easterly anomaly dominates the midlatitudes, enhancing the chance of a TC striking the EC coast. In other words, the notable reduction in the eastward component of the flow possibly prevents TCs from recurving or moving northeastward to the Japan region. Moreover, Figure 9B shows that the cyclonic anomaly along the EC coast tends to move in a southwest direction at around 30°*N*, which may prevent those TCs landfalling in EC from moving further north. This can explain why the range of TCs' landfalling latitudes tends to get smaller during the 41 years (Figures 3C–F).

Global SST variations contributing to changes in TCs' landfalls

Previous studies have shown that global SST anomalies can remotely influence WNP TC genesis (Du et al., 2011; Mei et al., 2015; Gao et al., 2018; Zhao et al., 2018; Gao et al., 2020). We then calculate the trends of global SST from 1980 to 2020 (Figure 10A), and the correlations between global SSTs and the number of TC landfalls over mainland China (Figure 10B). The results reveal that the TC landfall frequency over mainland China is significantly negatively correlated to the SSTs over the TIO, the tropical and high-latitude North Atlantic, and the tropical central-eastern Pacific (Figure 10B). Figure 10A shows that the SST has increased significantly in TIO, consistent with a pronounced warming trend over the ocean during the past several decades (Hoerling et al., 2004; Du and Xie, 2008; Roxy et al., 2014), which might be associated with the amplification impact of global warming (Gao et al., 2020). The TIO warming could induce atmospheric anomalies, including suppressed convection and an anomalous surface anticyclone, and further suppress WNP TC activity (Du et al., 2011). Significant negative correlations between the TC landfall frequency and the SSTs over most areas of the TNA (Figure 10B), and significant SST increase over the same ocean area (Figure 10A) can also be observed. This is in line with Gao et al. (2018), who suggested that warm SST anomalies in the TNA might suppress TC landfalls by regulating TC genesis location and frequency associated with modulated environmental conditions. Below-normal SSTs over the tropical central and eastern Pacific may be optimal for above-normal TC activity over the WNP (Figure 10B). However, the SST changes in the tropical central and eastern Pacific are not significant from 1980 to 2020 (Figure 10A). In addition, the number of landfalling TCs over mainland China may be linked to the PDO, as suggested in previous studies (Goh and Chan, 2010; Mei et al., 2015). The correlation between the July–October PDO index and the anomalous TC landfall frequency in mainland

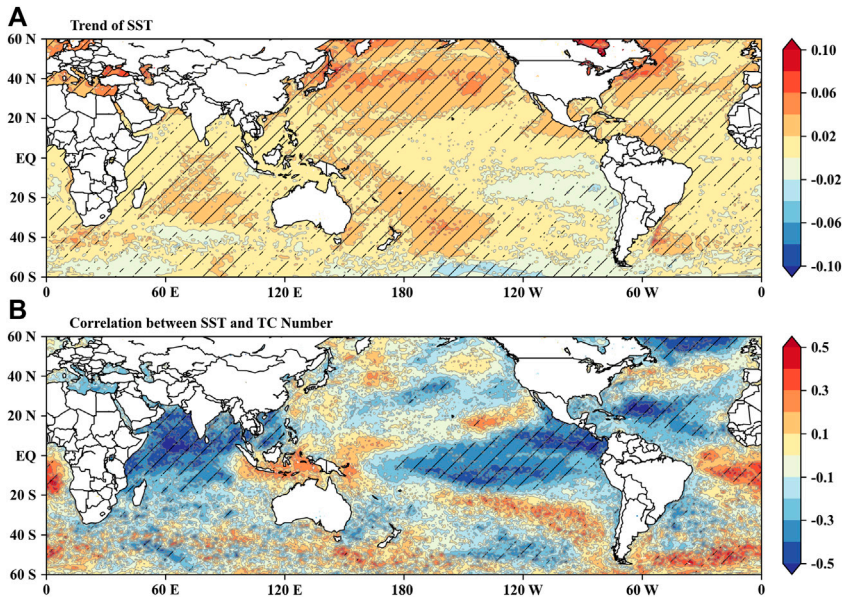

FIGURE 10
(A) Trends of global SST (°C yr^{-1}) from 1980 to 2020. **(B)** Correlations between global SSTs and the numbers of TCs making landfall in mainland China from 1980 to 2020. The striping indicates that the trends and correlations are statistically significant at the 90% confidence level.

China is -0.04, and it is not significant during the 41 years. It indicates that PDO has no apparent influence on the TCs' landfall frequency over mainland China.

Overall, the SST increases in the TIO, the tropical and high-latitude North Atlantic, and the tropical central and eastern equatorial Pacific may suppress the TC landfalls over mainland China from 1980 to 2020. During this period, the suppressing influence from the TIO may be more significant than the other ocean, due to its strong correlation with the TCs genesis and the consistent and universal SST increase.

Summary

This study examines the characteristics and variability of TC landfalls over mainland China from 1980 to 2020. Artificially, China is divided into SC and EC by the latitude line of 25°N. During the study period, 5.51 TCs land in SC, while 1.07 TCs land in EC annually. The number of TCs impacting mainland China decreases slightly from 1980 to 2020, the number of TCs landfalling in SC experiences a significant decrease, and there is no change in the number of TCs affecting EC. Based on the Pettitt's test results, the frequency of TCs' landfall in mainland China and SC appear to drop significantly in 1995/1996 and 1996/1997, respectively. From 1980 to 1995 (1996), the mean number of TCs landfalling over mainland China (SC) is 7.8 (6.6); from 1996 (1997) to 2020, the mean number of TCs landfalling over mainland China (SC) is 5.8 (4.8). The yearly mean of the TCs' landfalling latitudes moves northward slightly. Meanwhile, the maximum TCs' latitudes during the 4 decades are found to move southward slightly, leading to a slight decrease in the landfall latitudes range during the study period. All these landfall location shifts are not statistically significant. The significant reduction in the number of landfalling TCs over SC is mainly due to the apparent decrease in the frequency of TCs' formation in the WNP, which also indirectly leads to the markedly northwestward shift of the TC genesis region. The slight northward trend of the yearly mean TCs' landfalling latitude over mainland China is mainly due to the insignificant increase in their genesis latitudes.

The large-scale environments factors, including thermodynamic factors of PI and the middle troposphere RH, and the dynamic factors of lower-tropospheric absolute vorticity, VWS and steering flow, are investigated during the two periods, 1980–1995 and 1996–2020, to explore the environmental background contributing to the observed changes in the landfall and genesis of TCs influencing mainland China. It is found that the dynamic factors play a major role in the TCs' activity changes over the WNP in recent years. A large area of negative anomalies in the lower-tropospheric absolute vorticity and positive variations in the VWS over the tropical WNP, covering the major of the genesis region for TCs landfalling in China, suppresses TC formation over WNP. Concurrently, the opposite changes in both the low-level absolute vorticity and VWS over the northern region (north of 20°*N*) and southern region (south of 20°*N*) might contribute to the slight poleward shift of genesis locations of landfalling TCs during the 41 years.

In addition, the variation in the steering flow tends to result in a higher percentage of TCs making landfall along the eastern coast rather than the southern coast than before, with a slight southward shift in the maximum landfall latitudes for TCs. Finally, the SST increases in several ocean basins, the TIO, tropical and high-latitude North Atlantic, and the tropical central-eastern Pacific are found to suppress the formations of TCs that landfall in mainland China from 1980 to 2020. Among these oceans, TIO's influence is the greatest.

Data availability statement

Publicly available datasets were analyzed in this study. This data can be found here: http://tcdata.typhoon.org.cn/en/zjljsjj_zlhq.html https://cds.climate.copernicus.eu/#!/home https://psl.noaa.gov/data/climateindices/list/.

Author contributions

Conceptualization: QL and GL; data collection and analysis: GL; methodology: QL and GL; writing original draft: GL and QL; all the co-authors participated the manuscript review and editing.

Funding

This study was supported by the Science and Technology Department of Guangdong Province with Grant of 2019B111101002 and the Innovation of Science and Technology Commission of Shenzhen Municipality Ministry with Grants of JCYJ20210324101006016 and GJHZ20210705141403010.

Conflict of interest

The authors declare that the research was conducted in the absence of any commercial or financial relationships that could be construed as a potential conflict of interest.

Publisher's note

All claims expressed in this article are solely those of the authors and do not necessarily represent those of their affiliated organizations, or those of the publisher, the editors, and the reviewers. Any product that may be evaluated in this article, or claim that may be made by its manufacturer, is not guaranteed or endorsed by the publisher.

References

Bister, M., and Emanuel, K. A. (2002). Low frequency variability of tropical cyclone potential intensity 1. Interannual to interdecadal variability. *J. -Geophys. -Res.* 107 (D24), ACL 26-1–ACL 26-15. doi:10.1029/2001JD000776

Camargo, S. J., Emanuel, K. A., and Sobel, A. H. (2007). Use of a Genesis potential index to diagnose ENSO effects on tropical cyclone Genesis. *J. Clim.* 20 (19), 4819–4834. doi:10.1175/JCLI4282.1

Camargo, S. J., and Sobel, A. H. (2005). Western North Pacific tropical cyclone intensity and ENSO. *J. Clim.* 18 (15), 2996–3006. doi:10.1175/JCLI3457.1

Chan, J. C., and Gray, W. M. (1982). Tropical cyclone movement and surrounding flow relationships. *Mon. Weather Rev.* 110 (10), 1354–1374. doi:10.1175/1520-0493(1982)110<1354:TCMASF>2.0.CO;2

Chan, J. C. (1985). Identification of the steering flow for tropical cyclone motion from objectively analyzed wind fields. *Mon. weather Rev.* 113 (1), 106–116. doi:10.1175/1520-0493(1985)113<0106:IOTSFF>2.0.CO;2

Chan, J. C., Liu, K. S., Xu, M., and Yang, Q. (2012). Variations of frequency of landfalling typhoons in East China, 1450–1949. *Int. J. Climatol.* 32 (13), 1946–1950. doi:10.1002/joc.2410

Chen, X., Wu, L., and Zhang, J. (2011). Increasing duration of tropical cyclones over China. *Geophys. Res. Lett.* 38 (2). doi:10.1029/2010GL046137

Dong, S., Gao, J., Li, X., Wei, Y., and Wang, L. (2015). A storm surge intensity classification based on extreme water level and concomitant wave height. *J. Ocean. Univ. China* 14 (2), 237–244. doi:10.1007/s11802-015-2342-5

Du, Y., and Xie, S. P. (2008). Role of atmospheric adjustments in the tropical Indian Ocean warming during the 20th century in climate models. *Geophys. Res. Lett.* 35 (8), L08712. doi:10.1029/2008GL033631

Du, Y., Yang, L., and Xie, S.-P. (2011). Tropical Indian Ocean influence on northwest Pacific tropical cyclones in summer following strong El Niño. *J. Clim.* 24 (1), 315–322. doi:10.1175/2010JCLI3890.1

Emanuel, K. A. (2000). A statistical analysis of tropical cyclone intensity. *Mon. weather Rev.* 128 (4), 1139–1152. doi:10.1175/1520-0493(2000)128<1139:ASAOTC>2.0.CO;2

Emanuel, K. A. (1986). An air-sea interaction theory for tropical cyclones. Part I: Steady-state maintenance. *J. Atmos. Sci.* 43 (6), 585–605. doi:10.1175/1520-0469(1986)043<0585:AASITF>2.0.CO;2

Emanuel, K., and Nolan, D. S. (2004). "Tropical cyclone activity and the global climate system," in 26th Conference on Hurricanes and Tropical Meteorolgy, Miami, FL, 2-7 May (United States: American Meteorological Society).

Fudeyasu, H., Ito, K., and Miyamoto, Y. (2018). Characteristics of tropical cyclone rapid intensification over the Western North Pacific. *J. Clim.* 31 (21), 8917–8930. doi:10.1175/JCLI-D-17-0653.1

Gao, J., Zhao, H., Klotzbach, P. J., Wang, C., Raga, G. B., Chen, S., et al. (2020). Possible influence of tropical Indian Ocean sea surface temperature on the proportion of rapidly intensifying Western North Pacific tropical cyclones during the extended boreal summer. *J. Clim.* 33 (21), 9129–9143. doi:10.1175/JCLI-D-20-0087.1

Gao, S., Chen, Z., and Zhang, W. (2018). Impacts of tropical North Atlantic SST on Western North Pacific landfalling tropical cyclones. *J. Clim.* 31 (2), 853–862. doi:10.1175/JCLI-D-17-0325.1

Gilford, D. M., Solomon, S., and Emanuel, K. A. (2017). On the seasonal cycles of tropical cyclone potential intensity. *J. Clim.* 30 (16), 6085–6096. doi:10.1175/JCLI-D-16-0827.1

Goh, A. Z. C., and Chan, J. C. (2010). Interannual and interdecadal variations of tropical cyclone activity in the South China Sea. *Int. J. Climatol.* 30 (6), 827–843. doi:10.1002/joc.1943

Gray, W. M. (1968). Global view of the origin of tropical disturbances and storms. *Mon. Weather Rev.* 96 (10), 669–700. doi:10.1175/1520-0493(1968)096<0669:GVOTOO>2.0.CO;2

Gray, W. M. (1975). *Tropical cyclone genesis*. Colorado: Colorado State University.

Hersbach, H., Bell, B., Berrisford, P., Hirahara, S., Horányi, A., Muñoz-Sabater, J., et al. (2020). The ERA5 global reanalysis. *Q. J. R. Meteorol. Soc.* 146 (730), 1999–2049. doi:10.1002/qj.3803

Hoerling, M. P., Hurrell, J. W., Xu, T., Bates, G. T., and Phillips, A. (2004). Twentieth century North Atlantic climate change. Part II: Understanding the effect of Indian Ocean warming. *Clim. Dyn.* 23 (3), 391–405. doi:10.1007/s00382-004-0433-x

Holland, G. J. (1983). Tropical cyclone motion: Environmental interaction plus a beta effect. *J. Atmos. Sci.* 40 (2), 328–342. doi:10.1175/1520-0469(1983)040<0328:TCMEIP>2.0.CO;2

Kim, J.-H., Ho, C.-H., Kim, H.-S., Sui, C.-H., and Park, S. K. (2008). Systematic variation of summertime tropical cyclone activity in the Western North Pacific in relation to the Madden–Julian oscillation. *J. Clim.* 21 (6), 1171–1191. doi:10.1175/2007JCLI1493.1

Korty, R. L., Camargo, S. J., and Galewsky, J. (2012). Variations in tropical cyclone Genesis factors in simulations of the Holocene epoch. *J. Clim.* 25 (23), 8196–8211. doi:10.1175/JCLI-D-12-00033.1

Kossin, J. P., Emanuel, K. A., and Vecchi, G. A. (2014). The poleward migration of the location of tropical cyclone maximum intensity. *Nature* 509 (7500), 349–352. doi:10.1038/nature13278

Li, Q., and Duan, Y. (2010). Tropical cyclone strikes at the coastal cities of China from 1949 to 2008. *Meteorol. Atmos. Phys.* 107 (1), 1–7. doi:10.1007/s00703-010-0065-0

Li, R. C., Zhou, W., Shun, C., and Lee, T. C. (2017). Change in destructiveness of landfalling tropical cyclones over China in recent decades. *J. Clim.* 30 (9), 3367–3379. doi:10.1175/JCLI-D-16-0258.1

Ling, Z., Wang, Y., and Wang, G. (2016). Impact of intraseasonal oscillations on the activity of tropical cyclones in summer over the south China sea. Part I: Local tropical cyclones. *J. Clim.* 29 (2), 855–868. doi:10.1175/JCLI-D-15-0617.1

Liu, K., and Chan, J. C. (2003). Climatological characteristics and seasonal forecasting of tropical cyclones making landfall along the South China coast. *Mon. Weather Rev.* 131 (8), 1650–1662. doi:10.1175//2554.1

Liu, K. S., and Chan, J. C. (2013). Inactive period of Western North Pacific tropical cyclone activity in 1998–2011. *J. Clim.* 26 (8), 2614–2630. doi:10.1175/JCLI-D-12-00053.1

Liu, K. S., and Chan, J. C. (2020). Recent increase in extreme intensity of tropical cyclones making landfall in South China. *Clim. Dyn.* 55, 1059–1074. doi:10.1007/s00382-020-05311-5

Liu, K. S., and Chan, J. C. (2017). Variations in the power dissipation index in the East Asia region. *Clim. Dyn.* 48 (5), 1963–1985. doi:10.1007/s00382-016-3185-5

Liu, L., Wang, Y., Zhan, R., Xu, J., and Duan, Y. (2020). Increasing destructive potential of landfalling tropical cyclones over China. *J. Clim.* 33 (9), 3731–3743. doi:10.1175/JCLI-D-19-0451.1

Lu, X.-q., and Zhao, B.-k. (2013). Analysis of the climatic characteristics of landing tropical cyclones in East China. *J. Trop. Meteorology* 19 (2), 145.

Mei, W., Xie, S.-P., Zhao, M., and Wang, Y. (2015). Forced and internal variability of tropical cyclone track density in the Western North Pacific. *J. Clim.* 28 (1), 143–167. doi:10.1175/JCLI-D-14-00164.1

Murakami, H., Li, T., and Peng, M. (2013). Changes to environmental parameters that control tropical cyclone Genesis under global warming. *Geophys. Res. Lett.* 40 (10), 2265–2270. doi:10.1002/grl.50393

Park, D.-S. R., Ho, C.-H., and Kim, J.-H. (2014). Growing threat of intense tropical cyclones to East Asia over the period 1977–2010. *Environ. Res. Lett.* 9 (1), 014008. doi:10.1088/1748-9326/9/1/014008

Park, D.-S. R., Ho, C.-H., Kim, J.-H., and Kim, H.-S. (2013). Spatially inhomogeneous trends of tropical cyclone intensity over the Western North Pacific for 1977–2010. *J. Clim.* 26 (14), 5088–5101. doi:10.1175/JCLI-D-12-00386.1

Pettitt, A. N. (1979). A non-parametric approach to the change-point problem. *Appl. Stat.* 28 (2), 126. doi:10.2307/2346729

Roxy, M. K., Ritika, K., Terray, P., and Masson, S. (2014). The curious case of Indian ocean warming*, +. *J. Clim.* 27 (22), 8501–8509. doi:10.1175/JCLI-D-14-00471.1

Shan, K., and Yu, X. (2021). Variability of tropical cyclone landfalls in China. *J. Clim.* 34 (23), 9235–9247. doi:10.1175/JCLI-D-21-0031.1

Studholme, J., Fedorov, A. V., Gulev, S. K., Emanuel, K., and Hodges, K. (2022). Poleward expansion of tropical cyclone latitudes in warming climates. *Nat. Geosci.* 15 (1), 14–28. doi:10.1038/s41561-021-00859-1

Tippett, M. K., Camargo, S. J., and Sobel, A. H. (2011). A Poisson regression index for tropical cyclone Genesis and the role of large-scale vorticity in Genesis. *J. Clim.* 24 (9), 2335–2357. doi:10.1175/2010JCLI3811.1

Torn, R. D., Elless, T. J., Papin, P. P., and Davis, C. A. (2018). Tropical cyclone track sensitivity in deformation steering flow. *Mon. Weather Rev.* 146 (10), 3183–3201. doi:10.1175/MWR-D-18-0153.1

Wang, B., and Chan, J. C. (2002). How strong ENSO events affect tropical storm activity over the Western North Pacific. *J. Clim.* 15 (13), 1643–1658. doi:10.1175/1520-0442(2002)015<1643:HSEEAT>2.0.CO;2

Wang, H., Xu, M., Onyejuruwa, A., Wang, Y., Wen, S., Gao, A. E., et al. (2019). Tropical cyclone damages in Mainland China over 2005–2016: Losses analysis and implications. *Environ. Dev. Sustain.* 21 (6), 3077–3092. doi:10.1007/s10668-019-00481-7

Wang, S., and Toumi, R. (2021). Recent migration of tropical cyclones toward coasts. *Science* 371 (6528), 514–517. doi:10.1126/science.abb9038

Wang, Y. (2012). Recent research progress on tropical cyclone structure and intensity. *Trop. Cyclone Res. Rev.* 1 (2), 254–275. doi:10.6057/2012TCRR02.05

Wilks, D. S. (2006). *Statistical methods in the atmospheric sciences*. Cambridge: Academic Press.

Wu, L., and Wang, B. (2004). Assessing impacts of global warming on tropical cyclone tracks. *J. Clim.* 17 (8), 1686–1698. doi:10.1175/1520-0442(2004)017<1686:AIOGWO>2.0.CO;2

Wu, M., Wang, L., and Chen, B. (2020). Recent weakening in interannual variability of mean tropical cyclogenesis latitude over the Western North Pacific during boreal summer. *J. Meteorol. Res.* 34 (6), 1183–1198. doi:10.1007/s13351-020-0039-1

Yanase, W., Satoh, M., Taniguchi, H., and Fujinami, H. (2012). Seasonal and intraseasonal modulation of tropical cyclogenesis environment over the Bay of Bengal during the extended summer monsoon. *J. Clim.* 25 (8), 2914–2930. doi:10.1175/JCLI-D-11-00208.1

Yin, Y., Gemmer, M., Luo, Y., and Wang, Y. (2010). Tropical cyclones and heavy rainfall in Fujian Province, China. *Quat. Int.* 226 (1-2), 122–128. doi:10.1016/j.quaint.2010.03.015

Ying, M., Zhang, W., Yu, H., Lu, X., Feng, J., Fan, Y., et al. (2014). An overview of the China meteorological administration tropical cyclone database. *J. Atmos. Ocean. Technol.* 31 (2), 287–301. doi:10.1175/jtech-d-12-00119.1

Yonekura, E., and Hall, T. M.Climatology (2014). ENSO effect on East Asian tropical cyclone landfall via changes in tracks and Genesis in a statistical model. *J. Appl. Meteorol. Climatol.* 53 (2), 406–420. doi:10.1175/JAMC-D-12-0240.1

Zhan, R., Wang, Y., and Tao, L. (2014). Intensified impact of East Indian Ocean SST anomaly on tropical cyclone Genesis frequency over the Western North Pacific. *J. Clim.* 27 (23), 8724–8739. doi:10.1175/JCLI-D-14-00119.1

Zhan, R., and Wang, Y. (2017). Weak tropical cyclones dominate the poleward migration of the annual mean location of lifetime maximum intensity of Northwest Pacific tropical cyclones since 1980. *J. Clim.* 30 (17), 6873–6882. doi:10.1175/jcli-d-17-0019.1

Zhan, R., Wang, Y., and Wu, C.-C. (2011). Impact of SSTA in the East Indian ocean on the frequency of northwest pacific tropical cyclones: A regional atmospheric model study. *J. Clim.* 24 (23), 6227–6242. doi:10.1175/JCLI-D-10-05014.1

Zhang, Q., Zhang, W., Lu, X., and Chen, Y. D. (2012). Landfalling tropical cyclones activities in the South China: Intensifying or weakening? *Int. J. Climatol.* 32 (12), 1815–1824. doi:10.1002/joc.2396

Zhang, W., Vecchi, G. A., Murakami, H., Villarini, G., Delworth, T. L., Yang, X., et al. (2018). Dominant role of Atlantic multidecadal oscillation in the recent decadal changes in Western North Pacific tropical cyclone activity. *Geophys. Res. Lett.* 45 (1), 354–362. doi:10.1002/2017GL076397

Zhao, H., Duan, X., Raga, G., and Klotzbach, P. J. (2018). Changes in characteristics of rapidly intensifying Western North Pacific tropical cyclones related to climate regime shifts. *J. Clim.* 31 (19), 8163–8179. doi:10.1175/JCLI-D-18-0029.1